

## High performance InGaZnO thin film transistor with InGaZnO source and drain electrodes

Hung-Chi Wu and Chao-Hsin Chien

Citation: [Applied Physics Letters](#) **102**, 062103 (2013); doi: 10.1063/1.4789997

View online: <http://dx.doi.org/10.1063/1.4789997>

View Table of Contents: <http://scitation.aip.org/content/aip/journal/apl/102/6?ver=pdfcov>

Published by the [AIP Publishing](#)

---

### Articles you may be interested in

[Mobility enhancement in amorphous InGaZnO thin-film transistors by Ar plasma treatment](#)

*Appl. Phys. Lett.* **102**, 222103 (2013); 10.1063/1.4809727

[Electrical characterization of a-InGaZnO thin-film transistors with Cu source/drain electrodes](#)

*Appl. Phys. Lett.* **100**, 112109 (2012); 10.1063/1.3694273

[Correlation of photoconductivity response of amorphous In–Ga–Zn–O films with transistor performance using microwave photoconductivity decay method](#)

*Appl. Phys. Lett.* **98**, 102107 (2011); 10.1063/1.3561755

[Nitrogenated amorphous InGaZnO thin film transistor](#)

*Appl. Phys. Lett.* **98**, 052102 (2011); 10.1063/1.3551537

[Fully transparent InGaZnO thin film transistors using indium tin oxide/graphene multilayer as source/drain electrodes](#)

*Appl. Phys. Lett.* **97**, 172106 (2010); 10.1063/1.3490245

---

The advertisement features a dark blue background with white and orange text. At the top left, it reads 'NEW! Asylum Research MFP-3D Infinity™ AFM' in large white letters, followed by 'Unmatched Performance, Versatility and Support' in orange. On the right, the Oxford Instruments logo is shown with the tagline 'The Business of Science®'. Below the text are four images: a blue textured surface, a brown textured surface, a yellow and red patterned surface, and a photograph of the AFM instrument. Text descriptions are placed around these images: 'Stunning high performance' next to the blue surface, 'Simpler than ever to GetStarted™' next to the brown surface, 'Comprehensive tools for nanomechanics' next to the yellow and red patterned surface, and 'Widest range of accessories for materials science and bioscience' next to the photograph of the instrument.

# High performance InGaZnO thin film transistor with InGaZnO source and drain electrodes

Hung-Chi Wu<sup>1</sup> and Chao-Hsin Chien<sup>2,a)</sup>

<sup>1</sup>Department of Electronics Engineering and Institute of Electronics, National Chiao Tung University, Hsinchu, Taiwan

<sup>2</sup>Department of Electronics Engineering and Institute of Electronics, National Chiao Tung University, Hsinchu, Taiwan and National Nano Device Laboratories, Hsinchu, Taiwan

(Received 23 October 2012; accepted 17 January 2013; published online 11 February 2013)

This work demonstrates In-Ga-Zn-O (IGZO) as source and drain electrodes in IGZO-thin film transistors (TFTs). The fabricated TFT depicts excellent electrical properties; its mobility is 18.02 (cm<sup>2</sup>/V s), threshold voltage ( $V_{th}$ ) is 0.3 (V), on/off ratio is  $1.63 \times 10^8$  and subthreshold swing (S.S.) is 239 (mV/decade). We find using rapid thermal annealing treatment can convert IGZO into an effective conductor, and the transparency of IGZO remained almost unchanged. We also find sufficient thermal budget is needed for getting stable transfer curve and output characteristic; otherwise, current fluctuation in on-state can be easily observed. With IGZO electrodes, fully transparent IGZO-TFTs can be thus realized on a glass substrate. © 2013 American Institute of Physics. [<http://dx.doi.org/10.1063/1.4789997>]

Amorphous oxide semiconductors (AOS) have attracted industrial and commercial interests in recent years. Their advantages include low temperature process, large area fabrication, low cost, and compatibility with flexible electronics.<sup>1</sup> Its wide application to the flexible electronics, thin film transistors (TFTs), electronic papers, and sensors make AOS have the possibility to become the mainstream channel material for the next generation TFTs.<sup>2,3</sup> Among several AOS materials, In-Ga-Zn-O (IGZO) is one of the most promising candidates. The TFTs with IGZO usually exhibit more superior electrical properties than those with amorphous silicon, poly-silicon, and organic conjugated polymers in terms of channel mobility, on/off ratio, subthreshold swing (S.S.), and threshold voltage ( $V_{th}$ ).<sup>4,5</sup> Moreover, IGZO thin film is transparent since its plasma frequency lies in the infrared region.<sup>6</sup> This feature facilitates the production of transparent display, detectors, and other applications.<sup>7,8</sup> Even so, the IGZO-TFTs are not fully transparent since they need nontransparent metal as the source and drain electrodes. The presence of metal source and drain will certainly deteriorate the transparency since metals are opaque. Although indium-tin-oxide (ITO) is reported to be a good transparent electrode, the transparency of ITO is very sensitive to the process condition and post deposition treatment.

In this work, we demonstrate the possibility of making high performance IGZO-TFTs with IGZO source and drain electrodes. We find that rapid thermal annealing (RTA) can convert the IGZO thin film into an effective conductor. With sufficient thermal budget our fabricated IGZO-TFTs with IGZO source and drain electrodes depict excellent electrical properties in terms of mobility, threshold voltage, and on/off ratio. Certainly, the transparency has been improved by replacing metal source and drain electrodes. Our results suggest the fabrication of highly transparent IGZO-TFTs with non-metal electrodes is feasible.

Figure 1 shows the outline of process flow and the device structure. We used the bottom gate bottom contact structure, which is believed to be more suitable for the TFT technology than the bottom-gate top-contact structure, and it has also recently been proposed for a-IGZO TFTs.<sup>9</sup> After standard RCA cleaning, we used n<sup>++</sup> Si wafer as the substrate, and its backside was coated by Al as the gate electrode. The 200 nm SiO<sub>x</sub> layer was deposited by plasma enhanced chemical vapor deposition system (PECVD), and its capacitance was  $1.38 \times 10^{-8}$  F/cm<sup>2</sup>. Then, we deposited IGZO (IGZO-E) source and drain electrode regions (S/D) of 30 nm thickness by sputter and lithography. Next, the 30 nm IGZO channel region (IGZO-C) of width  $W = 200 \mu\text{m}$  and length  $L = 50 \mu\text{m}$  was defined and deposited by lithography and the following sputter. During sputter process, base and working pressure were  $2 \times 10^{-6}$  and  $7.6 \times 10^{-3}$  Torr, respectively. Ar/O<sub>2</sub> = 24/6 SCCM (SCCM denotes cubic centimeter per minute), DC power was 70 W. Before the IGZO-C deposition, we divided our sample into three categories. Sample A was the control one without thermal treatment for the

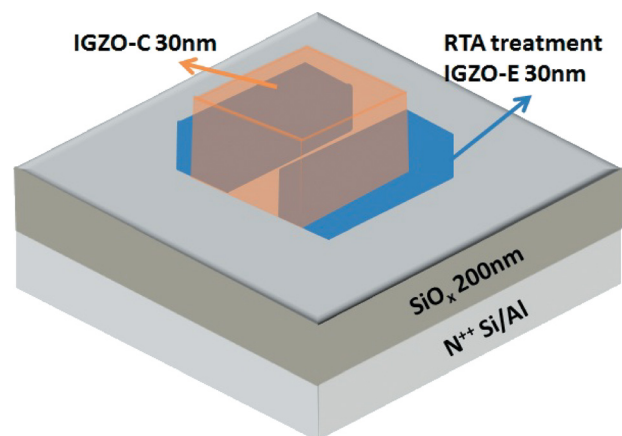
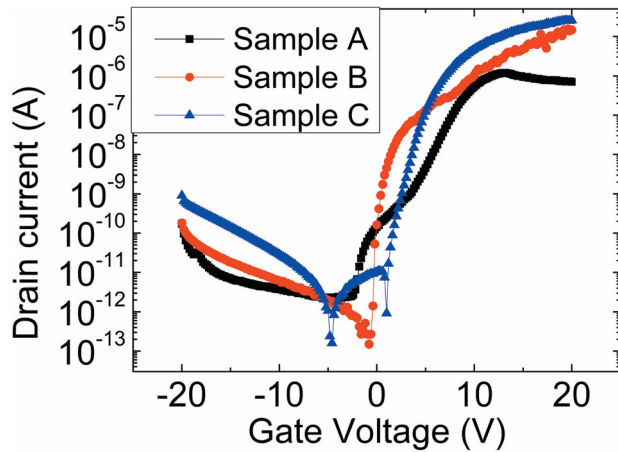


FIG. 1. The device structure (bottom gate and bottom contact). IGZO layers for different purposes are also marked.

<sup>a)</sup>Electronic mail: [chchien@faculty.nctu.edu.tw](mailto:chchien@faculty.nctu.edu.tw).

FIG. 2.  $I_D$ - $V_G$  transfer curves of samples A, B, and C.

IGZO-E, while sample B and C accepted RTA treatment in  $N_2$  ambient at  $400^\circ\text{C}$  before the deposition of IGZO-C. The durations for RTA treatment were 30 and 60 s, respectively.

The electrical properties were measured by HP4156 semiconductor parameter analyzer, the drain voltage was set to 5 V, and the gate voltage was swept from  $-20\text{ V}$  to  $20\text{ V}$ . We also measured its output characteristics with varying drain voltage from 0 V to 20 V and gate voltage 0 V to 20 V with a step of 5 V. The thin film properties such as the composition ratio and metal-oxygen bonding state was measured by X-ray photoelectron spectroscopy (XPS), the optical transmission measurement of the IGZO film was measured for wavelength ranging from 300 to 800 nm by ultraviolet/visible/near infrared spectroscopy, and Hall effect measurements were performed by Hall effect system at room temperature.

Figure 2 shows the transfer curves of samples. Table I summarizes the corresponding electrical parameters in this work and other IGZO TFTs with various S/D electrodes. We employed the current model of the conventional Si metal-oxide-semiconductor field-effect-transistor (MOSFET),<sup>15</sup> and the expression is as follows:

$$I_D = \frac{W_\mu C}{L} \left[ (V_G - V_{th})V_D - \frac{V_D^2}{2} \right] \quad (\text{linear regime}).$$

Hence the mobility was extracted according to  $\mu = \frac{L}{WCV_D} \frac{\partial I_D}{\partial V_G}$ . In addition, the S.S. was extracted from the linear portion of the transfer curve by

$$\text{S.S.} = \frac{\partial V_G}{\partial \log I_D},$$

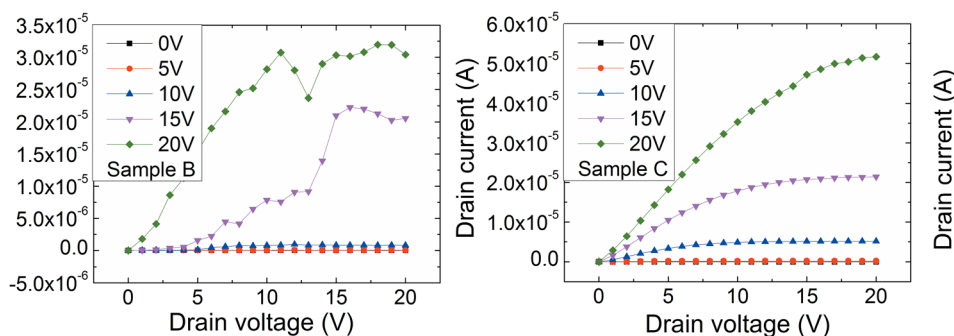
FIG. 3.  $I_D$ - $V_D$  output characteristics of sample B and C as a function of gate voltage.

TABLE I. Comparison of the various electrical parameters of our IGZO-TFTs with those of the reported IGZO-TFTs with various metal electrodes.

S/D material	$V_{th}$ (V)	Mobility ( $\text{cm}^2/\text{V s}$ )	S.S. (V/decade)	On/off ratio
IGZO sample A	-4.1	1.1	0.695	$4.42 \times 10^6$
IGZO sample B	-0.8	5.53	0.193	$9.42 \times 10^7$
IGZO sample C	0.3	18.02	0.239	$1.63 \times 10^8$
Cu <sup>10</sup>	N/A	8.3	0.43	$>10^8$
Mo <sup>11</sup>	4.87	8.9	0.096	$1.5 \times 10^{10}$
Ti/Au <sup>12</sup>	-0.92	10.2	0.13	$2.2 \times 10^6$
AZO <sup>13</sup>	0.6	13.7	0.25	$4.7 \times 10^6$
Mo/n <sup>+</sup> IGZO <sup>14</sup>	0.2	5	0.2	$\sim 10^7$

where  $W$  is the transistor channel width,  $L$  is the transistor channel length,  $C$  is the capacitance per unit area of the gate insulator ( $\text{SiO}_2$ ),  $\mu$  is the field-effect mobility,  $I_D$ ,  $V_D$ , and  $V_G$  are the drain current, drain, and gate voltage, respectively.

Sample A depicts acceptable  $V_{th}$  value and on/off ratio but poor S.S. Especially, the mobility is of only about  $1\text{ cm}^2/\text{V s}$ . Moreover, there is an abnormal current behavior between  $-3\text{ V}$  and  $10\text{ V}$  and a reduction of on-current with increased gate voltage. These results mean the carriers cannot be effectively injected from the electrode into the channel. However, sample B and C show steeper S.S., much higher mobility, which achieves the standard of IGZO application, and more impressive on/off ratio than sample A. Also, both sample B and C do not have the abnormal current behavior before the transistors are turned on. These results suggest that the RTA treatment can transform the IGZO-E into an effective conductor. As a result, we can make high performance IGZO-TFTs without metal source and drain electrodes. As compared with the reported IGZO-TFTs in Table I, we consider the properties of our devices are comparable with those of the conventional IGZO-TFTs with metal electrodes. This approach can obviously enhance the transparency of TFTs and, more importantly, is fully comparable with the conventional IGZO-TFT with metal electrodes processing. Fig. 3 shows  $I_D$ - $V_D$  output characteristics of sample B and C. We observe the curves of sample B are not very stable. There is apparent current oscillation at high gate and drain voltages. In contrast, sample C shows very stable and smooth curves at the whole applied voltage range. This implies that the duration of RTA shall be long enough to convert the IGZO-E into an effective conductor. In other words, the thermal budget shall be sufficient for well transformation of IGZO from a semiconductor into an effective conductor.

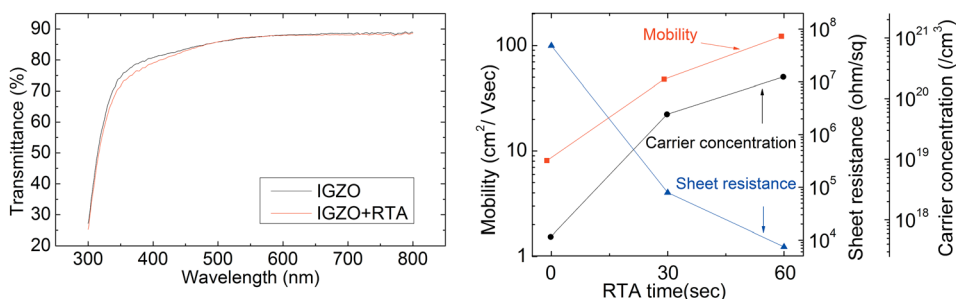


FIG. 4. Left: transmission spectra of IGZO thin films with and without RTA treatment (400 °C, 60 s). Right: carrier concentration, sheet resistance, and Hall mobility of IGZO film as a function of RTA treatment (400 °C) time.

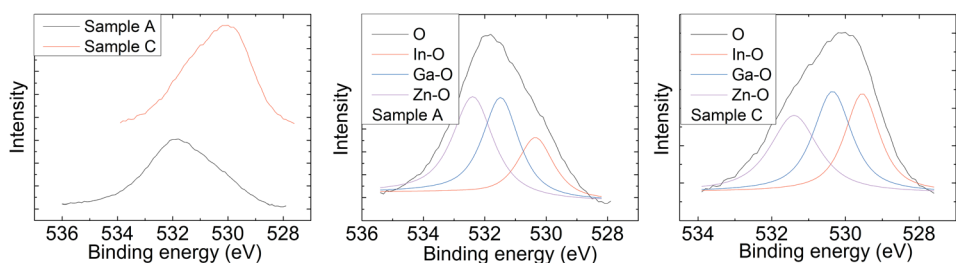


FIG. 5. O 1s XPS narrow scan spectra on the IGZO thin film surface with sample A (without any treatment) and sample C (with RTA treatment) and its bonding states analysis.

In Fig. 4, we show the optical transmittance spectra of the IGZO thin film with and without RTA treatment. We can observe there is no obvious change of optical transmittance of the IGZO film for all the wavelengths after the RTA treatment except around 300–450 nm. Even though the transmittance decreases around 300–450 nm, the film is still transparent with over 70% transmittance. In contrast, the transmittance of IGZO-TFTs with metal electrodes is typically under 10%. Therefore, we think using the RTA treated IGZO thin film as the electrodes is a good approach to show the feasibility of fully transparent IGZO-TFTs. The carrier concentration, sheet resistance, and Hall mobility of the IGZO films are also shown in Fig. 4. We can see both carrier concentration and Hall mobility of the RTA-treated IGZO film are higher than those of the IGZO film without RTA treatment and increase with the RTA duration. The carrier concentration of IGZO thin film can reach about the level of  $10^{20}$  (/cm<sup>3</sup>). Moreover, the sheet resistance reduces after the RTA treatment and decreases correspondingly with the prolonged RTA duration. This means the contact between the IGZO-E and IGZO-C can be improved, which is consistent with the results of the transfer and output characteristic curves of our devices. As a result, we confirm that the RTA treatment can significantly change the properties of IGZO and make the IGZO suitable for the transparent electrodes.

In order to identify the mechanism of conductivity modification of IGZO thin film by the RTA treatment, XPS analyses were also conducted. We observe that there is an obvious change in IGZO composition after the RTA treatment was performed (not shown). There is about two times increase on the amount of elements In, Ga, and Zn after RTA. Hence, we think the amount of oxygen reduction results from the oxygen out-diffusion during the RTA process. However, the composition change cannot thoroughly explain why the IGZO can be transferred into a conductor. Fig. 5 shows the XPS narrow scan spectra of the IGZO thin film with and without RTA treatment. From the result, we speculate the bonding states in the IGZO thin film will substantially influence the behavior of IGZO

thin film. We observe the signals for metal elements In, Ga, and Zn basically remain the same in samples A and C except the signal intensity (not shown); after RTA treatment, the intensities of signals for the metal elements increase which means the atom ratio of O is decrease. On the contrary, O spectrum shows the obvious signal shape difference between samples A and C, and the binding energy has shifted about 1.4 eV, indicating the bond state has been changed with the RTA treatment. It should be noted that all peaks have been calibrated referring to the carbon peak. We also deconvoluted the O XPS spectra into three waves representing for the indium(In), gallium(Ga), and zinc(Zn) oxide bonding states, as shown in Fig. 4. We find the indium oxide bonding state becomes stronger after RTA treatment as compared to the other oxide bonding states. Indium oxide has the highest electron density among three oxides so that we think indium oxide can supply more electron carriers.<sup>16</sup> The carrier concentration of a conventional IGZO film is usually below  $10^{21}$  (/cm<sup>3</sup>);<sup>17</sup> this fact means the IGZO is not metallic. However, the reduction in atom ratio of O in the IGZO thin film with the RTA treatment implies that many oxygen vacancies can be created. The oxygen vacancies were reported being able to provide more electrons and make the IGZO film behave like a conductor.<sup>18,19</sup>

Therefore, IGZO can act as an effective conductor after RTA treatment. We conclude the RTA treatment can change the bonding state situation in the IGZO thin film, increase the ratio of indium oxide bonding state, and result in more electron carrier generation.

In summary, we have investigated the feasibility of IGZO-TFTs without metal S/D electrodes. We find that the conductivity of IGZO thin film can be enhanced by a conventional RTA process without losing its transparency. High performance IGZO-TFTs with IGZO S/D electrodes were fabricated and demonstrated. We think the RTA treatment can change the situation of the oxide bonding states in IGZO thin film and convert IGZO from a semiconductor into a conductor. And we show the possibility of the fabrication of fully transparent IGZO TFTs.

- <sup>1</sup>K. Nomura, H. Ohta, A. Takagi, T. Kamiya, M. Hirano, and H. Hosono, *Nature (London)* **432**, 488 (2004).
- <sup>2</sup>E. Fortunato, P. Barquinha, A. Pimentel, A. Goncalves, A. Marques, L. Pereira, and R. Martins, *Adv. Mater.* **17**, 590 (2005).
- <sup>3</sup>R. L. Hoffman, B. H. Norris, and J. F. Wager, *Appl. Phys. Lett.* **82**, 733 (2003).
- <sup>4</sup>H. Yabuta, M. Sano, K. Abe, T. Aiba, T. Den, H. Kumomi, K. Nomura, T. Kamiya, and H. Hosono, *Appl. Phys. Lett.* **89**, 112123 (2006).
- <sup>5</sup>W. Lim, E. A. Douglas, S. H. Kim, D. P. Norton, S. J. Pearton, F. Ren, H. Shen, and W. H. Chang, *Appl. Phys. Lett.* **93**, 252103 (2008).
- <sup>6</sup>A. Solieman, *J. Sol-Gel Sci. Technol.* **60**, 48 (2011).
- <sup>7</sup>S. J. Kim, B. Kim, J. Jung, D. H. Yoon, J. Lee, S. H. Park, and H. J. Kim, *Appl. Phys. Lett.* **100**, 103702 (2012).
- <sup>8</sup>T. Kamiya, K. Nomura, and H. Hosono, *Sci. Technol. Adv. Mater.* **11**, 044305 (2010).
- <sup>9</sup>J. S. Park, W.-J. Maeng, H.-S. Kim, and J.-S. Park, *Thin Solid Films* **520**, 1679 (2012).
- <sup>10</sup>J. Jeong, G. J. Lee, J. Kim, and B. Choi, *Appl. Phys. Lett.* **100**, 112109 (2012).
- <sup>11</sup>L.-Y. Su, H.-Y. Lin, H.-K. Lin, S.-L. Wang, L.-H. Peng, and J. J. Huang, *IEEE Electron Device Lett.* **32**, 1245 (2011).
- <sup>12</sup>L. Yuan, X. Zou, G. Fang, J. Wan, H. Zhou, and X. Zhao, *IEEE Electron Device Lett.* **32**, 42 (2011).
- <sup>13</sup>X. Zou, G. Fang, J. Wan, N. Liu, H. Long, H. Wang, and X. Zhao, *Semicond. Sci. Technol.* **26**, 055003 (2011).
- <sup>14</sup>J. Park, I. Song, S. Kim, S. Kim, C. Kim, J. Lee, H. Lee, E. Lee, H. Yin, K.-K. Kim *et al.*, *Appl. Phys. Lett.* **93**, 053501 (2008).
- <sup>15</sup>S. M. Sze, *Physics of Semiconductor Devices* (Wiley, New York, 2006).
- <sup>16</sup>O. Bierwagen and J. S. Speck, *Appl. Phys. Lett.* **97**, 072103 (2010).
- <sup>17</sup>H. Hosono, *J. Non-Cryst. Solids* **352**, 851–858 (2006).
- <sup>18</sup>T.-C. Fung, C.-S. Chuang, C. Chen, K. Abe, R. Cottle, M. Townsend, H. Kumomi, and J. Kanicki, *J. Appl. Phys.* **106**, 084511 (2009).
- <sup>19</sup>B. D. Ahn, H. S. Shin, H. J. Kim, J.-S. Park, and J. K. Jeong, *Appl. Phys. Lett.* **93**, 203506 (2008).